JOURNAL OF VIROLOGY, Feb. 2003, p. 1977–1983 Vol. 77, No. 3
0022-538X/03/$08.00+0 DOI: 10.1128/JVI.77.3.1977–1983.2003

Two Retroviral Entry Pathways Distinguished by Lipid Raft Association of the Viral Receptor and Differences in Viral Infectivity

Shakti Narayan,[1,2] Richard J. O. Barnard,[2] and John A. T. Young[2]*

Cellular and Molecular Biology Program[1] and McArdle Laboratory for Cancer Research, Department of Oncology,[2] University of Wisconsin—Madison, Madison, Wisconsin 53706

Received 2 July 2002/Accepted 18 October 2002

The receptor "priming" model for entry of the retrovirus avian sarcoma and leukosis virus (ASLV) predicts that upon binding cell surface receptors, virions are endocytosed and trafficked to acidic endosomes where fusion occurs. To test this model directly, we have now followed subgroup A ASLV (ASLV-A) virions entering cells via either the transmembrane (TVA950) or glycophosphatidylinositol (GPI)-anchored (TVA800) forms of the cellular receptor. Our results suggest that viruses entering via these two forms of receptor are subjected to different intracellular fates, perhaps due to use of different endocytic trafficking pathways to access acidic fusion compartments. Kinetic analyses demonstrated that virus bound to TVA800 was taken up from the cell surface more slowly but then trafficked to the site of fusion more quickly than that entering via TVA950. Furthermore, transiently arresting virions within putative fusion compartments with NH_4Cl led to a substantially greater decrease in the infectivity of virions using TVA950 than with those using TVA800. The increased infectivity of virions using TVA800 correlated with the localization of this receptor to lipid rafts, since this effect was abolished by pharmacological disruption of lipid rafts. Together these results suggest that, in the presence of NH_4Cl, virus bound to the GPI-anchored receptor may utilize a lipid raft-dependent pathway to accumulate within a fusion compartment where it is more stable than if it enters via the transmembrane receptor. The TVA800/ASLV-A system should prove useful for the molecular analysis of lipid raft-dependent endocytosis and may provide a tool for the biochemical dissection of the poorly understood uncoating step of retroviral replication.

To initiate infection, the lipid bilayer of an enveloped virus must fuse with a cellular membrane for delivery of the viral nucleocapsid to the host cell cytoplasm. These events involve conversion of the viral envelope glycoprotein (Env) from its native, metastable state to its fusion-activated form, which represents its lowest energy state (7). Viral envelope glycoproteins are triggered to activate fusion either by pH-independent or pH-dependent mechanisms. Following virus uptake, low-pH-dependent viral glycoproteins are triggered by the acidic environment of an endosomal compartment. In contrast, pH-independent viral glycoproteins seem to be activated as a consequence solely of receptor interaction (7, 11).

Recent data obtained with the avian sarcoma and leukosis virus (ASLV) system have provided evidence for a third type of triggering mechanism in which receptor interaction converts (primes) the viral envelope protein so that it becomes sensitive to low-pH-induced activation (22). In support of this two-step model, ASLV entry is blocked by lysosomotropic agents that act to neutralize the low pH of endosomal compartments (15, 22). Also, ASLV Env-dependent cell-cell fusion leading to syncytium formation requires both receptor contact and a low-pH-induced activation signal. Moreover, low pH treatment abolishes the infectivity of soluble receptor-bound virions, generating thermostable sodium dodecyl sulfate (SDS)-resistant oligomers of the viral transmembrane subunit of Env, a property consistent with fusion activation (22).

The two-step model for ASLV entry predicts that following receptor binding and priming, virions are taken up into cells by endocytosis and then trafficked to an acidic endosomal compartment where fusion occurs (fusion compartment). Consistent with this notion, ASLV entry is blocked by expression of a dominant-negative dynamin-1 protein (22). To further explore this model of viral entry, we have now followed the fate of subgroup A ASLV (ASLV-A) virions that enter cells expressing either the transmembrane form or the glycophosphatidylinositol (GPI)-anchored form of TVA, the cellular receptor for ASLV-A (1, 37). The data obtained indicate that virions are taken up into cells and are trafficked to and escape from putative acidic fusion compartments with different kinetics depending upon the type of TVA receptor used. When infection of cells that express the GPI-linked TVA protein was transiently blocked with NH_4Cl, virions remained highly infectious. However, the same treatment of cells that express the transmembrane TVA receptor led to a striking loss of viral infectivity. This difference in viral infectivity correlated with association of the GPI-linked TVA protein with detergent-resistant membranes (DRMs) and indicates that ASLV-A can be trafficked to different intracellular compartments depending upon the nature of the receptor used.

* Corresponding author. Mailing address: McArdle Laboratory for Cancer Research, University of Wisconsin—Madison, 1400 University Ave., Madison, WI 53706. Phone: (608) 265-5151. Fax: (608) 262-2824. E-mail: young@oncology.wisc.edu.

MATERIALS AND METHODS

Chemicals and plasmid DNA. All chemicals were purchased from Sigma unless otherwise stated. Stock solutions of 500 mM NH_4Cl and 100 mM methyl-β-cyclodextrin (MβCD) were made in water and stored at 4°C and −20°C,

respectively. Fumonisin B1 stock solutions (5 mg/ml in dimethyl sulfoxide) were made just prior to use. The plasmids pCMMP (murine leukemia virus [MLV] vector), pCMMP EGFP, pMD.old.gagpol (encoding MLV Gag and Gag-Pol proteins), and pMD.G (encoding the vesicular stomatitis virus G protein) have been described previously (2, 28). The plasmid encoding Gαi-DsRed (13) was a generous gift from Bill Sugden (McArdle Laboratory, University of Wisconsin).

Cell lines and viruses. Human 293 cells were transduced with retroviral vectors that encode TVA950 or TVA800 (28). Briefly, the genes encoding these forms of TVA were subcloned into the MLV vector pCMMP. The resulting plasmids (pCMMP-TVA950 and pCMMP-TVA800) were then used in a tripartite transfection system along with plasmid pMD.old.gagpol and plasmid pMD.G as described previously (2). Virus-containing supernatants were then collected 48, 72, and 84 h posttransfection, pooled, and stored at −80°C after filter sterilization. These viruses were used to infect 293 cells, and expression of either TVA950 or TVA800 was subsequently confirmed 4 days later by flow cytometry using SUA-rIgG, a recombinant ASLV-A SU immunoglobulin G (rIgG) fusion protein, as described previously (38). The fluorescence-activated cell sorter-analyzed 293(TVA950) and 293(TVA800) cells expressed equivalent levels of cell surface receptors as judged by SUA-rIgG binding (data not shown). The vector RCASBP(A)-EGFP was used to generate ASLV-A virus stocks (35, 36).

Viral infections, citrate buffer, and NH_4Cl treatments. For infections, cells were rinsed once with Hank's balanced salt solution (HBSS) (Gibco) and dislodged from the plate with HBSS containing 5 mM EDTA at 37°C. An equal volume of ice-cold medium was added, and the cells were harvested by centrifugation at 1,000 × *g* for 5 min at 4°C. Cells were washed twice with ice-cold medium and then incubated with RCASBP(A)-EGFP at multiplicities of infection (MOIs) ranging from 0.8 to 2.8 enhanced green fluorescent protein (EGFP)-transducing units for 1 h at 4°C on a rocker (Nutator). Unbound virions were removed by rinsing with cold HBSS, and virus-cell complexes were transferred to ice-cold tissue culture plates. Infection was initiated (at a time designated as $t = 0$) by shifting the cells to 37°C. In the citrate buffer inactivation experiments, 10^6 virus-loaded cells were incubated at 37°C for the indicated times, returned to ice, and harvested by centrifugation at 14,000 × *g* for 1 min at 4°C. The cell pellet was resuspended in 1 ml of citrate buffer (pH 3.0) (14) and incubated for 2 min at room temperature to inactivate the surface-bound virions. The cells were then centrifuged at 14,000 × *g* for 1 min and washed twice with 1 ml of cold phosphate-buffered saline (PBS) (pH 7.4) and once with 1 ml of ice-cold medium. Cells were plated in a six-well tissue culture plate in 2 ml of medium and incubated at 37°C for 48 to 72 h. Samples were then analyzed by flow cytometry using a FACScalibur instrument (Becton Dickinson) to monitor EGFP expression in the infected cells (35). In the NH_4Cl inhibition experiments, either 7.5×10^5 cells/sample (for quantitative PCR [QPCR] analysis) or 4×10^5 cells/sample (for EGFP analysis) were used to create virus-loaded cells as described above. The NH_4Cl was added to medium at a final concentration of 30 mM at different time points and, where indicated, washed out by removing the medium and rinsing the cells with PBS (pH 7.4).

Quantification of viral entry by QPCR. The real-time QPCR experiments to detect early reverse transcription products were performed essentially as described previously (22). Late viral DNA products were quantified by a similar approach using the following primers: 5′ACCACTGAATTCCGCATTGC3′ (sense), 5′GGCCGACCACTATTCCCTAAC3′ (antisense), and 5′CCCTGAC GACTACGAGCACCTGCAT3′ (FAM Taqman probe; Perkin Elmer). A dilution series of RCASBP(A)-EGFP proviral DNA contained in a plasmid vector was used to construct a standard curve to quantify viral DNA. Routinely, between 10^2 and 10^7 DNA molecules were accurately measured by this assay (data not shown).

MβCD and Fumonisin B1 treatments. In the experiments involving MβCD treatment, 3×10^6 cells on 6-cm dishes were rinsed twice with serum-free medium (SFM) (prewarmed to 37°C) and treated at 37°C for 15 min with 2 ml of SFM containing 15 mM MβCD. The cells were then rinsed twice with prewarmed SFM, once with ice-cold SFM, and incubated at 4°C for 1 h with 2 ml of ice-cold SFM containing virus. Following removal of unbound virus with cold HBSS, cold medium was added and infection was initiated by shifting the cells to 37°C. NH_4Cl was added at the indicated times (i.e., $t = 0$ and $t = 60$ min) and 6 h later washed out as described above. Samples were analyzed after ~100 h by flow cytometry to monitor EGFP expression. In the Fumonisin B1 experiments, 10^5 cells in six-well tissue culture plates were incubated with 40 μg of Fumonisin B1-containing medium/ml for 60 h. Virus infection, NH_4Cl treatment, and EGFP expression analysis were carried out as described above, except that these experiments were performed at an MOI of 0.16 EGFP-transducing units (determined without inhibitor).

Fractionation of detergent-soluble and -insoluble membranes. 293(TVA950) or 293(TVA800) cells plated at 20 to 40% confluency on a 10-cm tissue culture plate were transfected with plasmid DNA encoding the lipid raft marker Gαi-DsRed (13) by calcium phosphate precipitation. Forty-eight hours later, 10^7 cells were washed once with ice-cold PBS and then twice with 37°C-prewarmed SFM. In MβCD extraction experiments, the cells were incubated for 15 min at 37°C with medium containing 15 mM MβCD. The medium was then removed and cells were chilled on ice prior to 30 min of incubation at 4°C with 2 ml of ice-cold lysis buffer (MBS buffer [25 mM morpholineethanesulfonic acid, 150 mM NaCl, pH 6.5] containing 0.5% Triton-X-100). The cell lysate was adjusted to 40% sucrose by addition of 2 ml of an 80% sucrose solution, and a 1-ml aliquot of this mixture was overlaid sequentially with 3.5 ml of 30% sucrose followed by 0.5 ml of 5% sucrose (all sucrose solutions were prepared in MBS). These samples were centrifuged at 240,000 × *g* for 18 h at 4°C in a Beckman SW55Ti rotor. Twelve equal fractions were collected from the sucrose gradient and were mixed in a 1:1 ratio with 2× SDS sample buffer, boiled, and subjected to SDS-polyacrylamide gel electrophoresis. Gαi-DsRed and TVA proteins were detected by Western blotting using a horseradish peroxidase-coupled secondary antibody (Amersham Pharmacia) and either an anti-DsRed antibody (catalog numbers 8370 to 8372; Clontech) or SUA-rIgG (38), respectively. TVA was quantitated in the different gradient fractions by quantitative Western blotting analysis using a ^{35}S-labeled anti-rabbit antibody (catalog number SJ424-50; Amersham). The resultant blots were exposed to a phosphorimaging screen for 48 to 80 h and analyzed using a Typhoon PhosphorImager and ImageQuant software (Molecular Dynamics).

RESULTS

TVA800 is associated with DRMs, but TVA950 is not. Previously, two forms of the TVA receptor were identified: TVA950 is a transmembrane form, whereas TVA800 is a GPI-anchored protein (1, 37). To characterize the viral entry mechanisms associated with each of these receptors, we first asked if either one or both is associated with DRMs (or lipid rafts). Lipid rafts are believed to be microdomains of cellular membranes that are rich in cholesterol, sphingolipids, and GPI-linked proteins (3, 34). Previous studies had indicated that the association of some viral receptors with lipid rafts was important for the efficiency of viral entry (for example, human immunodeficiency virus type 1 [17, 19, 31], ecotropic MLV [18], and simian virus 40 [29, 30]).

To test DRM association, TVA800- and TVA950-expressing cells were lysed in a Triton X-100-containing buffer at 4°C and subjected to flotation analysis by using a sucrose step gradient. Under these conditions, DRMs float toward the top of the gradient, whereas detergent-soluble fractions remain at the bottom (4, 8). Greater than 70% of the total TVA800 cofractionated with Gαi-DsRed, a coexpressed DRM-associated marker protein (Fig. 1A and C, fractions 9 to 11, and F). Moreover, like the marker protein, most of the TVA800 was solubilized when cells were treated with MβCD to disrupt DRMs by cholesterol extraction (Fig. 1B and D, fractions 1 to 4, and F). These data demonstrated that a substantial portion of TVA800 was associated with DRMs. By contrast, the TVA950 protein was found exclusively in the detergent-soluble fraction of cell membranes (Fig. 1E, lanes 1 to 4), and disruption of DRMs had no effect on the localization of TVA950 (data not shown). Therefore, the two TVA receptors seem to exist in different microdomains of cellular membranes.

TVA950 promotes faster virus uptake than does TVA800. Recently, several lipid raft-dependent endocytic pathways have been described that are distinct from classical clathrin-mediated endocytosis (12, 25). Thus, the DRM association of TVA800 but not TVA950 suggested that the viral entry properties associated with each of these receptors might be distinct. To explore this possibility, the rates of virus internalization in cells that express equivalent cell surface levels of TVA950 or

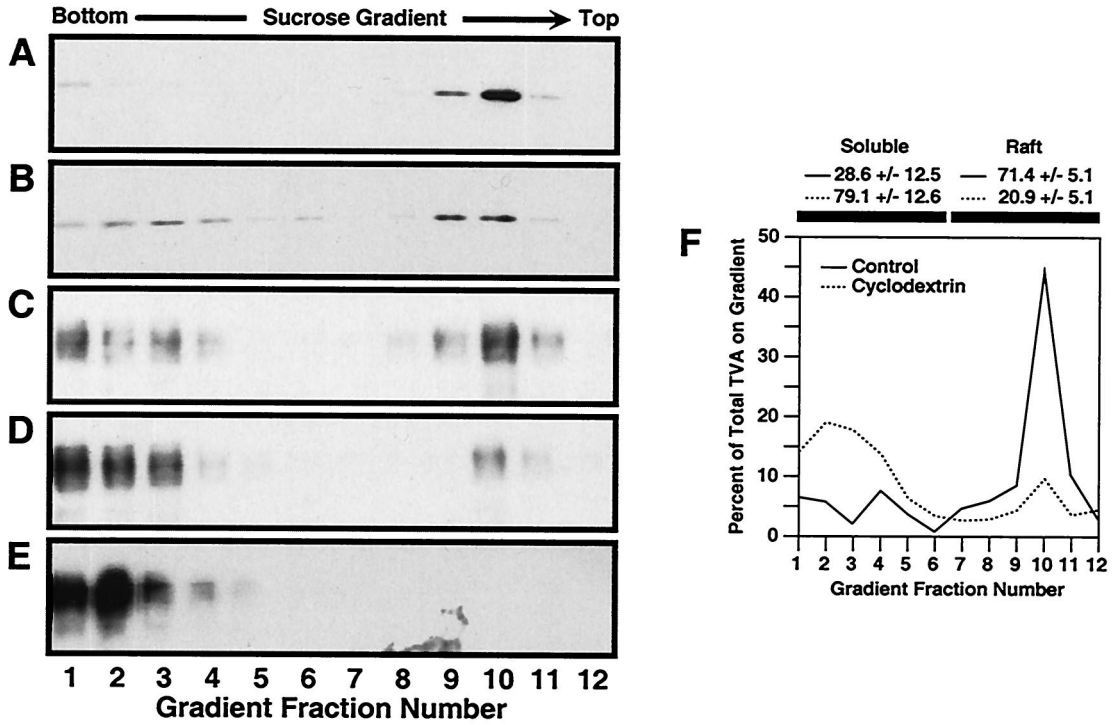

FIG. 1. TVA800 is associated with DRMs but TVA950 is not. Transfected human 293 cells expressing the lipid raft marker Gαi-DsRed and either TVA800 or TVA950 were either left untreated (A, C, and E) or were treated for 15 min at 37°C with 15 mM MβCD prior to ice-cold Triton X-100 lysis and sucrose gradient sedimentation (B and D). Fractions of each gradient were subjected to electrophoresis on a 12% polyacrylamide gel containing SDS followed by immunoblotting with an antibody specific for DsRed (13) (A and B) or with a subgroup A SU-immunoglobulin fusion protein (38) to detect TVA800 (C and D) or TVA950 (E). The relative levels of TVA800 in different fractions of the sucrose gradients prepared with samples from untreated or MβCD-treated cells (F) were measured using quantitative immunoblotting. The figure shown is representative of such an experiment. The mean and standard deviations of TVA800 levels in both soluble and lipid raft fractions were calculated from three independent experiments.

TVA800 was determined. ASLV-A virions encoding the EGFP were bound to cells at 4°C and then infection was initiated by shifting the temperature to 37°C. At different time points thereafter, residual surface-associated virions were inactivated by addition of a pH 3.0 citrate-containing buffer (14). The efficiency of subsequent viral infection was then determined using flow cytometric analysis to measure the proportion of EGFP-expressing cells. Under the conditions used, citrate buffer treatment inactivated approximately 80% of cell surface-associated virions (Fig. 2A, $t = 0$).

TVA950 mediated rapid virus uptake, reaching a maximal level only 5 min after initiating infection (Fig. 2A). By contrast, TVA800-dependent viral entry displayed slower kinetics, with only approximately 50% of the total virions internalized after 5 min and the remainder being internalized more slowly up to 15 min later (Fig. 2A). These data demonstrated that the rate of virion uptake was dependent upon the type of TVA receptor used.

Virions from the cell surface reach and exit a putative acidic endosomal fusion compartment with similar kinetics when entering via either TVA receptor. To determine how quickly virions bound to TVA950 or TVA800 at the cell surface are trafficked to and escape from a putative acidic endosomal fusion compartment(s), the time required for these viruses to become resistant to inhibition by NH_4Cl was determined. NH_4Cl is a lysosomotropic agent that causes a rapid elevation in endosomal pH, thus blocking low-pH-dependent cellular processes (26, 27). A 10-h treatment of cells with 30 mM NH_4Cl was initiated at different time points after beginning infection, and subsequent viral infection was quantified using a real-time PCR assay for reverse-transcribed DNA (QPCR). These studies showed that when NH_4Cl was added at the time of initiating infection or 10 min later, there was a complete block to infection of both cell types (Fig. 2B). By contrast, NH_4Cl addition at 20 min or later after initiating infection had a greatly reduced effect upon viral infectivity (Fig. 2B). Presumably at these later time points a fraction of the virus had proceeded beyond the low-pH-sensitive step of infection.

By subjecting these data to linear regression analysis, it was determined that virus became resistant to NH_4Cl treatment with a half time of 23 or 22 min when entering via TVA950 or TVA800, respectively (Fig. 2B). Interestingly, infection of both cell types resumed immediately after NH_4Cl withdrawal (Fig. 2C), indicating that virions may have fused upon reacidification of the endosomal compartment in which they were presumably trapped during the period of inhibitor treatment. Taken together, the data in Fig. 2 suggest that virus bound to TVA800 is taken up from the cell surface more slowly than that bound to TVA950, but the TVA800-associated particles are delivered to a putative acidic endosomal fusion compartment more quickly than those associated with TVA950.

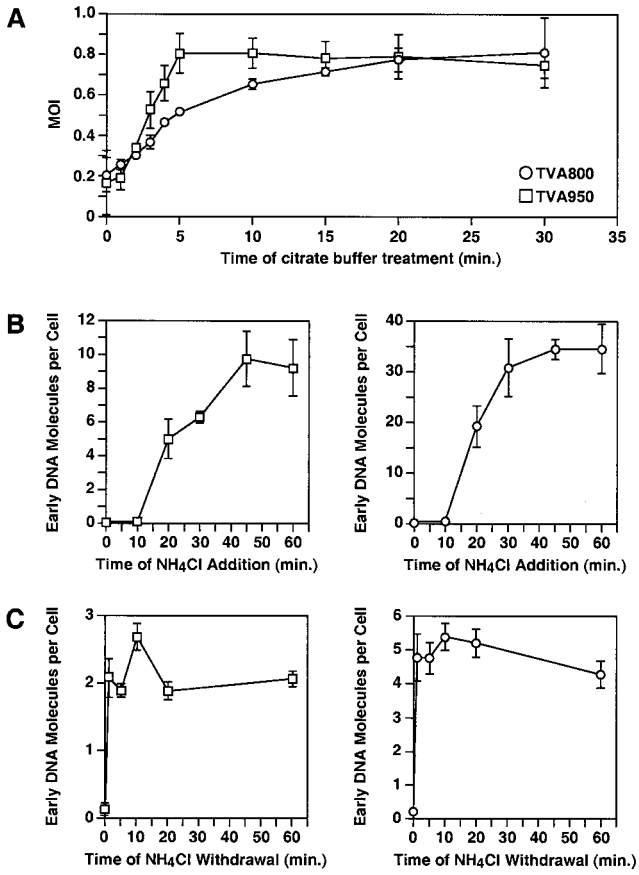

FIG. 2. Kinetics of viral uptake and trafficking via TVA950 and TVA800. An ASLV-A viral vector encoding EGFP [RCASBP(A)-EGFP] was bound on ice to transfected human 293 cells expressing either TVA950 (open squares) or TVA800 (open circles), and infection was then initiated by shifting the temperature to 37°C. (A) Internalization of ASLV-A virions from the cell surface via TVA800 and TVA950 occurs with different kinetics. At the different indicated time points after initiating infection, cells were treated with citrate buffer (pH 3.0) to inactivate surface-associated virions and infection of cells was subsequently determined by monitoring EGFP expression by flow cytometry. The MOI was calculated (in EGFP-transducing units) from the proportion of EGFP-positive cells (MOI = −ln [1 − (percent EGFP-positive cells/100)], and the combined results of four independent experiments with standard deviations are shown. (B) ASLV-A virions entering cells via either TVA950 or TVA800 reach the putative acidic fusion compartment with similar kinetics. At the different times indicated after initiating infection, 30 mM NH_4Cl was added for 10 h and then the amount of early viral DNA products generated was determined by real-time QPCR. A standard curve for enumeration was generated by using a dilution series of known amounts of proviral RCASBP(A)-EGFP DNA in a plasmid vector. Shown are representative experiments carried out at an MOI of 0.8 (TVA950) or 2.8 (TVA800) EGFP-transducing units. No significant kinetic differences were observed if cells expressing TVA800 were infected instead at an MOI of 0.02 EGFP-transducing units (data not shown). Error bars represent the standard deviations of the data. (C) ASLV-A virions resume infection immediately upon removal of NH_4Cl. After blocking infection for 6 h with 30 mM NH_4Cl, the inhibitor was washed out for the times indicated before the cells were placed again in medium containing the inhibitor for approximately 11 h. The number of early reverse transcription products that had been generated in each cell population was then determined as described in the legend to panel B. A representative experiment of three independent experiments done in triplicate is shown. Error bars represent standard deviations of the data.

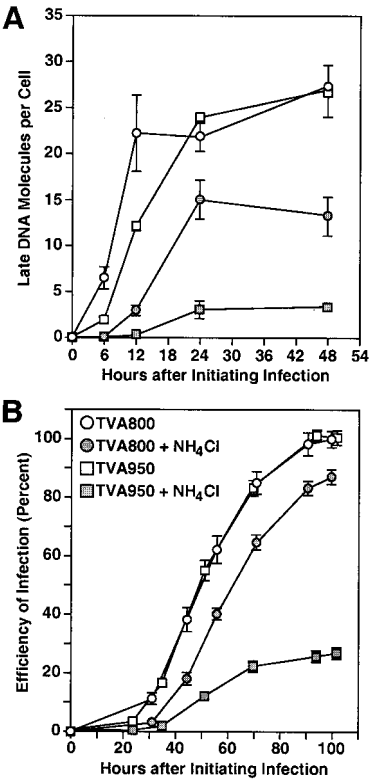

FIG. 3. NH_4Cl-arrested virions remain highly infectious when they use the TVA800 but not the TVA950 receptor. RCASBP(A)-EGFP was bound to transduced 293 cells expressing either TVA800 (circles) or TVA950 (squares), and infection was initiated either in the absence (open symbols) or presence (closed symbols) of a 6-h block by 30 mM NH_4Cl treatment. (A) At the indicated time points, the number of late reverse transcription products synthesized was determined as described in the legend to Fig. 2B. (B) A similar experiment was performed, but this time the number of resultant EGFP-positive cells was determined by flow cytometry at the indicated time points after initiating infection. These values were used to determine the efficiency of infection, defined as a percentage of that seen with untreated cells (MOI = 1.5 EGFP-transducing units). Representative experiments of three independent experiments that were each performed in triplicate are shown. Error bars represent the standard deviations of the data.

NH_4Cl-arrested virions in TVA800-expressing cells remain highly infectious, whereas those in TVA950-expressing cells do not. When following the fate of virions after NH_4Cl withdrawal by QPCR analysis of viral DNA products, a striking difference was seen in the residual level of viral infectivity between cells expressing either TVA800 or TVA950 (Fig. 3A). Viral infection was completely arrested in both cell types during the 6-h period of inhibitor treatment (Fig. 3A). However, upon NH_4Cl release, the level of subsequent infection seen with TVA800-expressing cells was approximately 60% of that seen with an untreated cell population (Fig. 3A). By contrast, the number of viral DNA products generated in the TVA950-expressing cell population was only 10% of that seen with untreated cells (Fig. 3A). These data indicated that NH_4Cl-arrested virions remain highly infectious in TVA800-expressing cells but not in TVA950-expressing cells.

The previous experiment monitored viral infectivity by measuring the quantity of viral DNA products produced in the infected cell population. However, only 20% of the viral DNA

made after infection remains stably integrated as proviral DNA in these cells (data not shown). Therefore, to monitor the fate of the infectious virions (i.e., those that go on to establish proviral DNA), a similar experiment was performed as that shown in Fig. 3A except that the expression of the virus-encoded EGFP was assessed as a measure of infectivity. The results obtained were strikingly similar to those obtained by the quantitative reverse transcription assay. Specifically, the efficiency of infection obtained with NH_4Cl-treated cells expressing either TVA800 or TVA950 was 85 and 20%, respectively, of that seen with untreated cells (Fig. 3B). Increasing the time of NH_4Cl treatment to 12 h caused a further decrease in infectivity of virions entering via TVA950 but did not affect those entering via TVA800 (data not shown). Together, these results demonstrated that NH_4Cl-arrested virions are much more stable in cells that express TVA800 as opposed to TVA950.

Disruption of DRMs markedly alters the stability of NH_4Cl-arrested virions in cells that express TVA800. To test whether TVA800 association with DRMs is responsible for the increased relative stability of NH_4Cl-arrested virions, cells expressing this receptor were treated with either MβCD or Fumonisin B1 (a sphingolipid biosynthesis inhibitor that also disrupts DRMs) (6). Cyclodextrin treatment by itself had only a minor effect on viral infectivity regardless of which TVA receptor was used for entry (Fig. 4A and C). However, when combined with a 6-h NH_4Cl block imposed at the time of initiating infection, this treatment led to a 50% loss of infectivity for virus entering via TVA800 (compare Fig. 4A and 3B). This loss of viral infectivity was largely overcome when NH_4Cl was instead added 60 min after initiating infection (Fig. 4A), a time when presumably a substantial fraction of virions had bypassed the low-pH-sensitive step (Fig. 2B). Similar results were obtained when cells were treated with Fumonisin B1 (Fig. 4B). To ensure that this cyclodextrin effect was specific for cells expressing the GPI-linked receptor, the same experiment was performed with TVA950-expressing cells. In this case, the NH_4Cl treatment led to the same (approximately 80%) decrease in viral infectivity irrespective of whether cyclodextrin had been added or not (compare Fig. 4B with 3B). Thus, the reduced level of viral infectivity that was seen by combining ammonium chloride and cyclodextrin treatments was specific for the TVA800-expressing cells. Together, these data indicate that the increased stability of NH_4Cl-arrested virions in TVA800-expressing cells, relative to that seen with TVA950-expressing cells, closely correlates with the association of the GPI-linked receptor with DRMs.

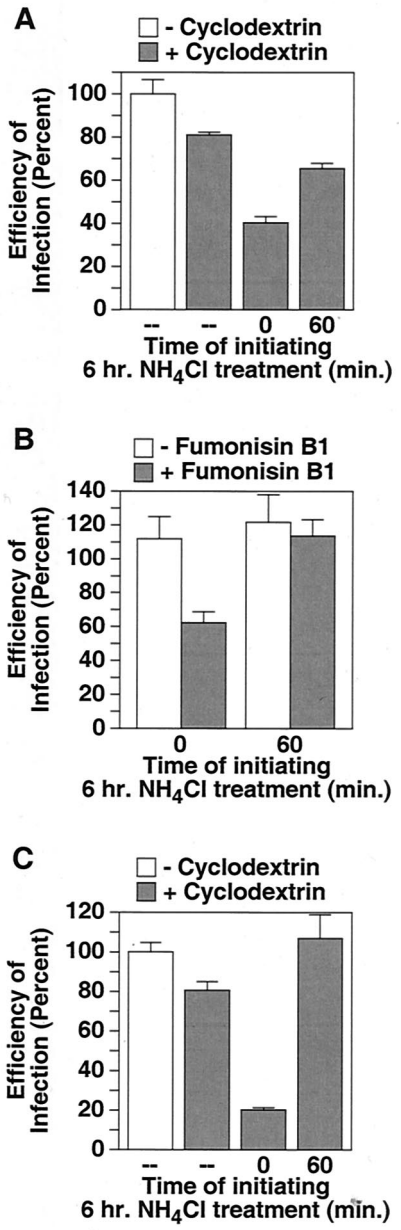

FIG. 4. Disruption of DRMs leads to a loss of infectivity of NH_4Cl-arrested virions in TVA800-expressing cells but not in cells expressing TVA950. To disrupt DRMs, human 293 cells expressing TVA800 (A) or TVA950 (C) were treated for 15 min with SFM containing 15 mM MβCD, 293 cells expressing TVA800 were treated with 40 μg of Fumonisin B1/ml for 60 h (B), or the cells were left untreated before challenge with RCASBP(A)-EGFP. Where indicated, a 6-h block to infection was imposed with 30 mM NH_4Cl added just prior to ($t = 0$) or 60 min after ($t = 60$) initiating infection. The number of resultant EGFP-positive cells was determined by flow cytometry ~100 h after initiating infection. The efficiency of infection is shown as a percentage of that level obtained with untreated cells (MOI = 1.6 [A], 0.16 [B], and 1.4 [C] EGFP-transducing units). In each case, a representative experiment performed in triplicate is shown. Error bars represent the standard deviations of the data.

DISCUSSION

Previously, our laboratory proposed a model in which ASLV enters cells by receptor-mediated endocytosis followed by low-pH-dependent fusion from an intracellular compartment (22). In the present report, we further substantiate this model and provide evidence that ASLV-A virions associated with a transmembrane form of the TVA receptor are internalized more rapidly than those using a GPI-anchored form of the receptor. However, virions become resistant to inhibition by the lysosomotropic agent NH_4Cl at similar rates regardless of which TVA receptor is used to enter the cells. Since these NH_4Cl experiments measure the combined kinetics of the initial uptake and the subsequent trafficking of virus particles, the simplest model to explain these data would be that upon being internalized, virions associated with the GPI-anchored recep-

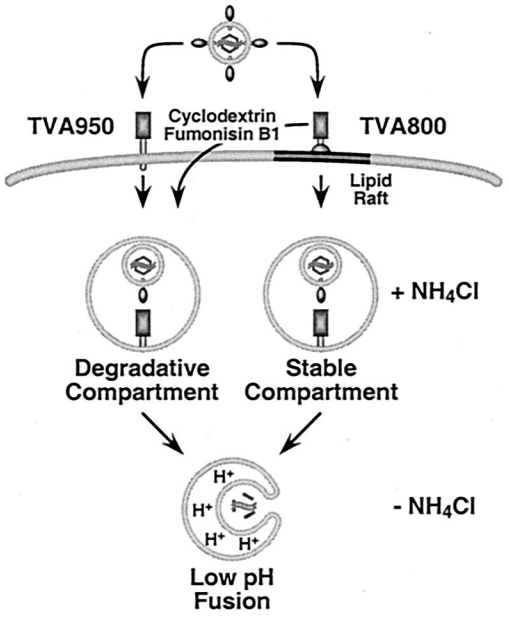

FIG. 5. Model for ASLV-A entry via transmembrane and GPI-anchored receptors. Virions bound to TVA950 are predicted to be taken up into cells by endocytosis and, in the presence of NH_4Cl, accumulate in a degradative compartment. In contrast, virions bound to TVA800 are predicted to utilize a lipid raft-dependent endocytic pathway and accumulate within a fusion compartment where they remain stable. Disruption of lipid rafts leads to viral accumulation in a degradative compartment instead. Infection resumes immediately after NH_4Cl withdrawal, suggesting that virions may fuse directly with membranes of the endosomes in which they are trapped during inhibitor treatment.

tor are subsequently trafficked to a putative fusion compartment more rapidly than those using the transmembrane-anchored form.

Remarkably, most virions that entered cells expressing TVA800 remained highly infectious in the presence of NH_4Cl, whereas those entering TVA950-expressing cells did not. This difference between the two types of TVA receptors correlated with the lipid raft association of the majority of the TVA800 protein. These data suggest that association of the receptor with lipid rafts influences the intracellular fate of virions (Fig. 5). The simplest model to explain these findings is that virions entering via TVA950 are trafficked via a degradative endocytic pathway that may involve multivesicular bodies, late endosomes, and lysosomes (10, 23). In contrast, virions entering cells via lipid raft-associated TVA800 may be endocytosed by a known, or as-yet-unknown, lipid raft-dependent endocytic pathway to a stable compartment. The loss of viral infectivity that was seen with NH_4Cl-treated TVA800-expressing cells (Fig. 3) may be due either to some intrinsic property of this "stable" compartment or, instead, might be due to virion uptake by receptors that reside outside of lipid rafts, which perhaps traffic the virus to a degradative compartment similar to that accessed by TVA950. We presently cannot distinguish between these two possibilities.

Consistent with our model, lipid raft-associated components seem to avoid the degradative endocytic pathway by being sorted into the recycling endosome, which contains a low level of endocytic proteases (9). Furthermore, some GPI-anchored proteins, such as folate receptor and CD55, are endocytosed and trafficked through this recycling endosome (6, 21, 33). Alternatively, TVA800-associated virions may use another lipid raft-dependent endocytic pathway, such as that used by CD59, which traffics directly between the plasma membrane and the Golgi apparatus (24); that used by simian virus 40, a nonenveloped virus which enters cells via caveolae and accesses the endoplasmic reticulum via the caveosome, a novel sorting organelle (29, 30); or that used by the interleukin-2 receptor, which seems to be independent of these other endocytic pathways (16). It is also possible that in the presence of NH_4Cl, virions bound to TVA800 and TVA950 are trafficked to different "domains" of the same intracellular compartment. In support of this idea, it was recently suggested that proteins targeted for degradation may be localized to the internal invaginations of late endosomes, while those found at the outer limiting membrane are poorly degradable (10). The use of pathway-specific inhibitors as well as quantitative imaging techniques to track individual virions may help distinguish between these various models of viral entry.

By characterizing the entry pathway used by ASLV-A, we hope not only to gain a better understanding of the mechanism by which this retrovirus enters cells but also to obtain new insights into how lipid raft-associated cargo is taken up into cells and delivered to an acidic endosomal compartment. To date, there has not been much information available on how such cargo is trafficked to an acidic endosome. This information, in turn, may help us better understand the entry mechanisms of other viruses that use GPI-anchored receptors, such as Jaagsiekte sheep retrovirus (32) and perhaps Ebola virus (5). In addition, the fact that we can stably arrest ASLV-A infection in TVA800-expressing cells by using NH_4Cl is a novel finding, since low-pH-dependent viruses are generally unstable under these conditions, presumably because they have been delivered to a degradative compartment (20). This feature of the ASLV system may allow for the isolation of virus-containing endosomes which, upon reacidification, may support virus-cell membrane fusion. If so, this system could allow for a detailed biochemical analysis of receptor priming, fusion, and of the poorly defined subsequent step of viral uncoating that leads to reverse transcription.

ACKNOWLEDGMENTS

We thank Ajamete Kaykas and Bill Sugden for advice on biochemical analysis of lipid rafts, Kristin Ostrow for help with quantitative immunoblotting, Paul Ahlquist for comments on the manuscript, John Naughton for help with figures, and members of the Young lab for sharing reagents and comments on the manuscript.

This work was supported by NIH grant CA70810.

REFERENCES

1. **Bates, P., J. A. Young, and H. E. Varmus.** 1993. A receptor for subgroup A Rous sarcoma virus is related to the low density lipoprotein receptor. Cell **74:**1043–1051.
2. **Boerger, A. L., S. Snitkovsky, and J. A. Young.** 1999. Retroviral vectors preloaded with a viral receptor-ligand bridge protein are targeted to specific cell types. Proc. Natl. Acad. Sci. USA **96:**9867–9872.
3. **Brown, D. A., and E. London.** 1998. Functions of lipid rafts in biological membranes. Annu. Rev. Cell Dev. Biol. **14:**111–136.
4. **Chamberlain, L. H., R. D. Burgoyne, and G. W. Gould.** 2001. SNARE proteins are highly enriched in lipid rafts in PC12 cells: implications for the spatial control of exocytosis. Proc. Natl. Acad. Sci. USA **98:**5619–5624.
5. **Chan, S. Y., C. J. Empig, F. J. Welte, R. F. Speck, A. Schmaljohn, J. F.**

Kreisberg, and M. A. Goldsmith. 2001. Folate receptor-alpha is a cofactor for cellular entry by Marburg and Ebola viruses. Cell **106:**117–126.
6. **Chatterjee, S., E. R. Smith, K. Hanada, V. L. Stevens, and S. Mayor.** 2001. GPI anchoring leads to sphingolipid-dependent retention of endocytosed proteins in the recycling endosomal compartment. EMBO J. **20:**1583–1592.
7. **Eckert, D. M., and P. S. Kim.** 2001. Mechanisms of viral membrane fusion and its inhibition. Annu. Rev. Biochem. **70:**777–810.
8. **Fra, A. M., E. Williamson, K. Simons, and R. G. Parton.** 1994. Detergent-insoluble glycolipid microdomains in lymphocytes in the absence of caveolae. J. Biol. Chem. **269:**30745–30748.
9. **Gagescu, R., N. Demaurex, R. G. Parton, W. Hunziker, L. A. Huber, and J. Gruenberg.** 2000. The recycling endosome of Madin-Darby canine kidney cells is a mildly acidic compartment rich in raft components. Mol. Biol. Cell **11:**2775–2791.
10. **Gruenberg, J.** 2001. The endocytic pathway: a mosaic of domains. Nat. Rev. Mol. Cell. Biol. **2:**721–730.
11. **Hernandez, L. D., L. R. Hoffman, T. G. Wolfsberg, and J. M. White.** 1996. Virus-cell and cell-cell fusion. Annu. Rev. Cell Dev. Biol. **12:**627–661.
12. **Ikonen, E.** 2001. Roles of lipid rafts in membrane transport. Curr. Opin. Cell Biol. **13:**470–477.
13. **Kaykas, A., K. Worringer, and B. Sugden.** 2001. CD40 and LMP-1 both signal from lipid rafts but LMP-1 assembles a distinct, more efficient signaling complex. EMBO J. **20:**2641–2654.
14. **Kizhatil, K., and L. M. Albritton.** 1997. Requirements for different components of the host cell cytoskeleton distinguish ecotropic murine leukemia virus entry via endocytosis from entry via surface fusion. J. Virol. **71:**7145–7156.
15. **Knauss, D. J., and J. A. Young.** 2002. A fifteen-amino-acid TVB peptide serves as a minimal soluble receptor for subgroup B avian leukosis and sarcoma viruses. J. Virol. **76:**5404–5410.
16. **Lamaze, C., A. Dujeancourt, T. Baba, C. G. Lo, A. Benmerah, and A. Dautry-Varsat.** 2001. Interleukin 2 receptors and detergent-resistant membrane domains define a clathrin-independent endocytic pathway. Mol. Cell **7:**661–671.
17. **Liao, Z., L. M. Cimakasky, R. Hampton, D. H. Nguyen, and J. E. Hildreth.** 2001. Lipid rafts and HIV pathogenesis: host membrane cholesterol is required for infection by HIV type 1. AIDS Res. Hum. Retrovir. **17:**1009–1019.
18. **Lu, X., and J. Silver.** 2000. Ecotropic murine leukemia virus receptor is physically associated with caveolin and membrane rafts. Virology **276:**251–258.
19. **Manes, S., G. del Real, R. A. Lacalle, P. Lucas, C. Gomez-Mouton, S. Sanchez-Palomino, R. Delgado, J. Alcami, E. Mira, and A. C. Martinez.** 2000. Membrane raft microdomains mediate lateral assemblies required for HIV-1 infection. EMBO Rep. **1:**190–196.
20. **Marsh, M., and A. Helenius.** 1989. Virus entry into animal cells. Adv. Virus Res. **36:**107–151.
21. **Mayor, S., S. Sabharanjak, and F. R. Maxfield.** 1998. Cholesterol-dependent retention of GPI-anchored proteins in endosomes. EMBO J. **17:**4626–4638.
22. **Mothes, W., A. L. Boerger, S. Narayan, J. M. Cunningham, and J. A. Young.** 2000. Retroviral entry mediated by receptor priming and low pH triggering of an envelope glycoprotein. Cell **103:**679–689.
23. **Mukherjee, S., R. N. Ghosh, and F. R. Maxfield.** 1997. Endocytosis. Physiol. Rev. **77:**759–803.
24. **Nichols, B. J., A. K. Kenworthy, R. S. Polishchuk, R. Lodge, T. H. Roberts, K. Hirschberg, R. D. Phair, and J. Lippincott-Schwartz.** 2001. Rapid cycling of lipid raft markers between the cell surface and Golgi complex. J. Cell Biol. **153:**529–541.
25. **Nichols, B. J., and J. Lippincott-Schwartz.** 2001. Endocytosis without clathrin coats. Trends Cell Biol. **11:**406–412.
26. **Ohkuma, S., and B. Poole.** 1981. Cytoplasmic vacuolation of mouse peritoneal macrophages and the uptake into lysosomes of weakly basic substances. J. Cell Biol. **90:**656–664.
27. **Ohkuma, S., and B. Poole.** 1978. Fluorescence probe measurement of the intralysosomal pH in living cells and the perturbation of pH by various agents. Proc. Natl. Acad. Sci. USA **75:**3327–3331.
28. **Ory, D. S., B. A. Neugeboren, and R. C. Mulligan.** 1996. A stable human-derived packaging cell line for production of high titer retrovirus/vesicular stomatitis virus G pseudotypes. Proc. Natl. Acad. Sci. USA **93:**11400–11406.
29. **Pelkmans, L., J. Kartenbeck, and A. Helenius.** 2001. Caveolar endocytosis of simian virus 40 reveals a new two-step vesicular-transport pathway to the ER. Nat. Cell Biol. **3:**473–483.
30. **Pelkmans, L., D. Puntener, and A. Helenius.** 2002. Local actin polymerization and dynamin recruitment in SV40-induced internalization of caveolae. Science **296:**535–539.
31. **Popik, W., T. M. Alce, and W. C. Au.** 2002. Human immunodeficiency virus type 1 uses lipid raft-colocalized CD4 and chemokine receptors for productive entry into $CD4^+$ T cells. J. Virol. **76:**4709–4722.
32. **Rai, S. K., F. M. Duh, V. Vigdorovich, A. Danilkovitch-Miagkova, M. I. Lerman, and A. D. Miller.** 2001. Candidate tumor suppressor HYAL2 is a glycosylphosphatidylinositol (GPI)-anchored cell-surface receptor for Jaagsiekte sheep retrovirus, the envelope protein of which mediates oncogenic transformation. Proc. Natl. Acad. Sci. USA **98:**4443–4448.
33. **Sabharanjak, S., P. Sharma, R. G. Parton, and S. Mayor.** 2002. GPI-anchored proteins are delivered to recycling endosomes via a distinct cdc42-regulated, clathrin-independent pinocytic pathway. Dev. Cell **2:**411–423.
34. **Simons, K., and D. Toomre.** 2000. Lipid rafts and signal transduction. Nat. Rev. Mol. Cell. Biol. **1:**31–39.
35. **Snitkovsky, S., T. M. Niederman, B. S. Carter, R. C. Mulligan, and J. A. Young.** 2000. A TVA-single-chain antibody fusion protein mediates specific targeting of a subgroup A avian leukosis virus vector to cells expressing a tumor-specific form of epidermal growth factor receptor. J. Virol. **74:**9540–9545.
36. **Snitkovsky, S., T. M. Niederman, R. C. Mulligan, and J. A. Young.** 2001. Targeting avian leukosis virus subgroup A vectors by using a TVA-VEGF bridge protein. J. Virol. **75:**1571–1575.
37. **Young, J. A., P. Bates, and H. E. Varmus.** 1993. Isolation of a chicken gene that confers susceptibility to infection by subgroup A avian leukosis and sarcoma viruses. J. Virol. **67:**1811–1816.
38. **Zingler, K., and J. A. Young.** 1996. Residue Trp-48 of Tva is critical for viral entry but not for high-affinity binding to the SU glycoprotein of subgroup A avian leukosis and sarcoma viruses. J. Virol. **70:**7510–7516.